

REFERENCES

- [1] Sharke, P. Freedom of Choice. *Mechanical Engineering* 126(2004) : 33.
- [2] Parsons, I., Solid oxide fuel cell. *Fuel Cell Handbook*, Fifth Edition ed.; U.S.Department of Energy Office of Fossil Energy: Morgantown, 2000; p 1.
- [3] Varga, Á.; Mounsey, S. Solid Oxide Fuel Cell. http://www.doitpoms.ac.uk/tlplib/fuel-cells/sofc_electrolyte.php. (accessed 5 January 2008).
- [4] Rao, C. N. R.; Gopalakrishnan, J.; Vidyasagar, K. Superstructure, Ordered Defects and Nonstoichiometry in Metal Oxides of Perovskite and related Structure. *Indian Journal of Chemistry* 23A(4)(1984) : 265-284.
- [5] Yang, X.; Zhu, J.; Zhao, Z.; Xiao, D.; Li, J.; Wu, Y. Study of $\text{La}_{2-x}\text{Sr}_x\text{CuO}_4$ ($x = 0.0, 0.5, 1.0$) catalysts for NO+CO reaction from the measurements of O_2 -TPD, H_2 -TPR and cyclic voltammetry. *Journal of Molecular catalysis A: Chemical* 238(2005): 35–40.
- [6] Teraoka, Y.; Nobunaga, T.; Yamazoe, N. Effect of cation substitution on the oxygen semipermeability of perovskite-type oxide. *Chemistry Letters* (1988): 503-506.
- [7] Duan, Z.; Yang, M.; Yan, A.; Hou, Z.; Dong, Y.; Chong, Y.; Cheng, M.; Yang, W. $\text{Ba}_{0.5}\text{Sr}_{0.5}\text{Co}_{0.8}\text{Fe}_{0.2}\text{O}_{3-\delta}$ as a cathode for IT-SOFCs with a GDC interlayer. *Journal of Power Sources* 160(2006): 57–64.
- [8] Yamazoe, N.; Teraoka, Y.; Seiyama, T. TPD and XPS Study on Thermal Behavior of Adsorbed Oxygen in $\text{La}_{1-x}\text{Sr}_x\text{CoO}_3$. *Chemistry Letters* (1981): 1767.
- [9] Yokoi, Y.; Uchida, H. Catalytic Activity of Perovskite-Type Oxide Catalysts for Direct Decomposition of NO: Correlation Between Cluster Model Calculations and Temperature-Programmed Desorption Experiments. *Catalysis Today* 42(1998): 167-174.
- [10] Wikipedia, c. Nanotechnology. <http://en.wikipedia.org/w/index.php?title=Nanotechnology&oldid=282248221> (accessed 5 January 2008).

- [11] Wikipedia, c. Nanomaterials. <http://en.wikipedia.org/w/index.php?title=Nanomaterials&oldid=281735859> (accessed 5 January 2008).
- [12] Nagamoto, H.; Hayashi, K.; Inoue, H. Methane Oxidation by Oxygen Transported Through Solid Electrolyte. *Journal of Catalysis* 126 (1990): 671-673.
- [13] Wikipedia, c. Sol-gel. <http://en.wikipedia.org/w/index.php?title=Sol-gel&oldid=281892977> (accessed 5 January 2008).
- [14] Wikipedia, c. Hydrothermal synthesis. http://en.wikipedia.org/w/index.php?title=Hydrothermal_synthesis&oldid=268181006 (accessed 5 January 2008).
- [15] Richerson, D. W. *Modern Ceramic Engineering, Properties, Processing, and Use in Design*, 2nd ed., p378-381, 1992.
- [16] Kuczynski, G. C. Transactions of the American Institute of Mining, Metallurgical, and Petroleum Engineering. *Journal of Applied Physics* 21(1950) : 632-637.
- [17] Kharton, V. V.; Viskup, A. P.; Yaremchenko, A. A., Ionic conductivity of La(Sr)Ga(Mg,M)O_{3-δ} (M=Ti, Cr, Fe, Co, Ni): effects of transition metal dopants. *Solid State Ionics* **2000**, 132, 119-130.
- [18] Yang, W.; Shao, Z.; Cong, Y., Investigation of the permeation behavior and stability of a Ba_{0.5}Sr_{0.5}Co_{0.8}Fe_{0.2}O_{3-δ} oxygen membrane. *Journal of Membrane Science* **2000**, 172, 177-188.
- [19] Shankar, S. K.; Kar, S.; Subbanna, G. N., Enhanced ferromagnetic transition temperature in nanocrystalline lanthanum calcium manganese oxide (La_{0.67}Ca_{0.33}MnO₃). *Solid State Communications* **2004**, 129, 479-483.
- [20] Boskovic', B. S.; Matovic, Z. B.; Vlajic', D. M., Modified glycine nitrate procedure (MGNP) for the synthesis of SOFC nanopowders. *Ceramics International* **2007**, 33, 89-93.
- [21] Calder'on-Moreno, M. J.; Le, H. T. N.; Popa, M., LaNiO₃ nanopowder prepared by an 'amorphous citrate' route. *Journal of the European Ceramic Society* **2006**, 26, 403-407.

- [22] Ianculescu, A.; Berger, D.; Viviani, M., Investigation of $Ba_{1-x}Sr_xTiO_3$ ceramics prepared from powders synthesized by the modified Pechini route. **2007**, *27*, 3655–3658.
- [23] Ishihara, T.; Enoki, M.; Yan, J., High oxide ion conductivity in Fe and Mg doped $LaGaO_3$ as the electrolyte of solid oxide fuel cells. *Solid State Ionics* **2006**, *177*, 2053–2057.
- [24] Polini, R.; Falsetti, A.; Traversa, E., Sol–gel synthesis, X-ray photoelectron spectroscopy and electrical conductivity of Co-doped (La, Sr)(Ga, Mg) $O_{3-\delta}$ perovskites. *Journal of the European Ceramic Society* **2007**, *27*, 4291–4296.
- [25] Wang, W.; Nie, H.; Wang, S., $A_{2-\delta}A'_\deltaBO_4$ -type oxides as cathode materials for IT-SOFCs (A=Pr, Sm; A'=Sr; B=Fe, Co). *Materials Letters* **2006**, *60*, 1174–1178.
- [26] Huang, D.; Xu, Q.; Zhang, F., Synthesis and electrical conductivity of $La_2NiO_{4+\delta}$ derived from a polyaminocarboxylate complex precursor. *Materials Letters* **2006**, *60*, 1892–1895.
- [27] Li, T.; Wang, Z.; Jiang, S., Synthesis and characterization of $Ba_{1-x}Sr_xTiO_3$ nanopowders by citric acid gel method. *Ceramics International* **2006**, *xxx*, xxx-xxx.
- [28] Adschiri, T.; Hakuta, Y.; Sue, K., Hydrothermal synthesis of metal oxide nanoparticles at supercritical conditions. *Journal of Nanoparticle Research* **2001**, *227*–235.
- [29] Suchanek, W. L.; Riman, R. E., Hydrothermal Synthesis of Advanced Ceramic Powders. *Advances in Science and Technology* **2006**, *45*, 184-193.
- [30] Ishihara, T.; Ando, M.; Enoki, M., Oxide ion conductivity in $La(Sr)Ga(Fe,Mg)O_3$ and its application for solid oxide fuel cells. *Journal of Alloys and Compounds* **2006**, *408*–412, 507–511.
- [31] Ishihara, T.; Tabuchi, J.; Ishikawa, S., Recent progress in $LaGaO_3$ based solid electrolyte for intermediate temperature SOFCs. *Solid State Ionics* **2006**, *177*, 1949–1953.

- [32] Yang, W.; Chang, Y.; Huang, S., Influence of molar ratio of citric acid to metal ions on preparation of $\text{La}_{0.67}\text{Sr}_{0.33}\text{MnO}_3$ materials via polymerizable complex process. *Journal of the European Ceramic Society* **2005**, *25*, 3611–3618.
- [33] Lee, K. T. Effect of cation doping on the physical properties and electrochemical performance of $\text{Nd}_{0.6}\text{Sr}_{0.4}\text{Co}_{0.8}\text{M}_{0.2}\text{O}_{3-\delta}$ (M=Ti, Cr, Mn, Fe, Co, and Cu) cathodes. *Solid State Ionics* **2006**, *178*, 995–1000.
- [34] Subramania, A.; Saradha, T.; Muzhumathi S. Synthesis of nano-crystalline $(\text{Ba}_{0.5}\text{Sr}_{0.5})\text{Co}_{0.8}\text{Fe}_{0.2}\text{O}_{3-\delta}$ cathode material by a novel sol–gel thermolysis process for IT-SOFCs. *Journal of Power Sources* **2007**, *165*, 728–732.
- [35] Kharton, V. V.; Figueiredo, F. M.; Kovalevsky, A. V., Processing, microstructure and properties of $\text{LaCoO}_{3-\delta}$ ceramics. *Journal of the European Ceramic Society* **2001**, *21*, 2301–2309.
- [36] Kharton, V. V.; Marques, F. M. B., Mixed ionic–electronic conductors: effects of ceramic microstructure on transport properties. *Current Opinion in Solid State and Materials Science* **2002**, *6*, 261–269.
- [37] Tai, L. W.; Nasrallah, M. M.; Anderson, H. U.; Sparlin, D. M.; Sehlin, S. R. Structure and electrical properties of $\text{La}_{1-x}\text{Sr}_x\text{Co}_{1-y}\text{Fe}_y\text{O}_3$ Part 1. The system $\text{La}_{0.8}\text{Sr}_{0.2}\text{Co}_{1-y}\text{Fe}_y\text{O}_3$. *Solid State Ionics* **1995**, *76*, 259–27.
- [38] Li, S.; Lü, Z.; Huang, X.; Su, W. Thermal, electrical, and electrochemical properties of Nd-doped $\text{Ba}_{0.5}\text{Sr}_{0.5}\text{Co}_{0.8}\text{Fe}_{0.2}\text{O}_3$ as a cathode material for SOFC *Solid State Ionics* **2008**, *178*, 1853–1858.
- [39] Shao, Z.; Xiong, G.; Tong, J.; Dong, H.; Yang, W. Ba effect in doped $\text{Sr}(\text{Co}_{0.8}\text{Fe}_{0.2})\text{O}_{3-\delta}$ on the phase structure and oxygen permeation properties of the dense ceramic membranes. *Separation and Purification Technology* **2001**, *25*, 419–429.
- [40] Wang, Y.; Nie, H.; Wang, S., $\text{A}_{2-\alpha}\text{A}'_{\alpha}\text{BO}_4$ -type oxides as cathode materials for IT-SOFCs (A=Pr, Sm; A'=Sr; B=Fe, Co). *Materials Letters* **2006**, *60*, 1174–1178.

- [41] Wen, T.-L.; Nie, H. W.; Wang, S. R., Preparation, thermal expansion, chemical compatibility, electrical conductivity and polarization of $A_{2-\alpha}A'_{\alpha}MO_4$ ($A=Pr, Sm; A'=Sr; M=Mn, Ni; \alpha=0.3, 0.6$) as a new cathode for SOFC. *Solid State Ionics* **2006**, *177*, 1929–1932.
- [42] Kharton, V. V.; Shaula, A. L.; Yaremchenko, A. A., Oxygen permeability of $LaGaO_3$ -based ceramic membranes. *Journal of Membrane Science* **2003**, *221*, 69–77.
- [43] Dai, H.; Niu, J.; Deng, J., Nanosized perovskite-type oxides $La_{1-x}Sr_xMO_{3-\delta}$ ($M = Co, Mn; x = 0, 0.4$) for the catalytic removal of ethyl acetate. *Catalysis Today* **2007**, *126*, 420–429.
- [44] Ngampeungpis, W., Effects of doping metal ions on structures and properties of perovskites $Ba_{0.5}Sr_{0.5}Co_{0.8}Fe_{0.2}O_{3-\delta}$. *A Master Thesis*, Department of Chemistry, Faculty of Science, Chulalongkorn University, 2007.
- [45] Supanwanich, N., Structures and properties of strontium ion doped $Ln(Pr, La)_2(Co, Ni, Cu)O_4$ perovskites. *A Master Thesis*, Department of Chemistry, Faculty of Science, Chulalongkorn University, 2007.

APPENDICES

APPENDICES**APPENDICE A****Table A.1** Atomic weight, ionic charge, coordination number, and ionic radius of concerned metals[46]

Element	Charge	Ionic radius
Ba	2+	1.750
Sr	2+	1.580
Co	2+	0.890
Co	3+	0.750
Co	4+	0.670
Fe	2+	0.920
Fe	3+	0.785
Fe	4+	0.725
Ni	2+	0.830
Ni	3+	0.700
Ni	4+	0.620
Mg	2+	0.860
Ga	3+	0.760
Pr	3+	1.319
La	3+	1.500
O	2-	1.260

APPENDICE B

Activation Energy (E_a)

Arrhenius plot of H-BSCF- H_5 is given in Figure B-1. The linear part can be described by the small polaron conduction mechanism, following the formula:

$$\sigma = (A/T) e^{(-E_a/RT)} \quad \text{B.1}$$

$$\ln(\sigma T) = \ln A e^{(-E_a/RT)}$$

$$\ln(\sigma T) = \ln e^{(-E_a/RT)} + \ln A \quad \text{B.2}$$

A is material constant including the carrier concentration term,

σ = The specific conductivity (S/cm)

E_a = The activation energy (kJ/mol)

T = Temperature (K)

R = The gas constant = 8.314472 J/K.mol

From Equation B.2 Arrhenius plot of $\ln \sigma T$ versus $1000/T$ gives a straight line, whose slope and intercept can be used to determine E_a and A .

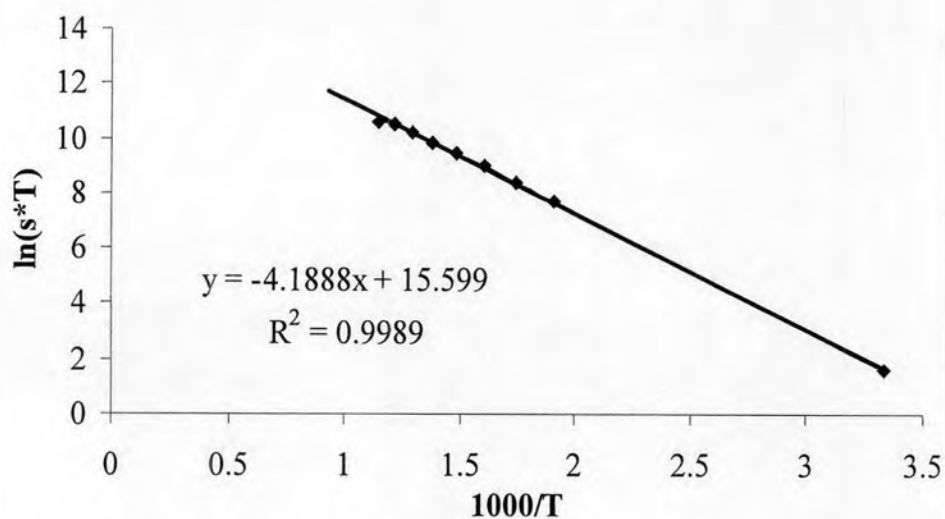


Figure B.1 Arrhenius plot of the electrical conductivity of H-BSCF- H_5

The activation energy calculated from the slope of the straight line of figure B.1 For example, the activation energy (E_a) of $\text{Pr}_2\text{Ni}_{0.7}\text{Cu}_{0.3}\text{O}_4$, was calculated as below:

$$\text{Slope} = -E_a/k$$

$$\text{Slope} = -E_a / 8.314472$$

$$E_a = -\text{slope} \times 8.314472$$

$$E_a = -(-4.1888) \times 8.314472$$

$$E_a = 34.83 \text{ kJ/mol}$$

APPENDICE C

Table C.1 Specific conductivity of $\text{Ba}_{0.5}\text{Sr}_{0.5}\text{Co}_{0.8}\text{Fe}_{0.2}\text{O}_3$ synthesized by sol gel method using various chelating agents

Sample	Specific conductivity, σ (S/cm)						
	27°C	250°C	300°C	350°C	400°C	450°C	500°C
S-BSCF-MC	0	$5.3 \pm 1.5 \times 10^{-1}$	$11.0 \pm 5.4 \times 10^{-2}$	$19.0 \pm 2.3 \times 10^{-1}$	$27.8 \pm 3.3 \times 10^{-1}$	37.5 ± 0	$46.7 \pm 3.6 \times 10^{-2}$
S-BSCF-G	0	$3.5 \pm 3.5 \times 10^{-2}$	$7.7 \pm 1.9 \times 10^{-1}$	$13.3 \pm 1.8 \times 10^{-1}$	20.4 ± 0	$28.6 \pm 6.0 \times 10^{-2}$	$37.5 \pm 9.4 \times 10^{-3}$
S-BSCF-H ₅	0	$4.7 \pm 5.4 \times 10^{-2}$	$9.8 \pm 1.1 \times 10^{-1}$	$15.7 \pm 1.9 \times 10^{-1}$	$22.7 \pm 2.4 \times 10^{-1}$	$31.1 \pm 7.7 \times 10^{-2}$	$40.7 \pm 1.2 \times 10^{-1}$
S-BSCF-GC	0	$4.0 \pm 5.7 \times 10^{-2}$	$9.6 \pm 3.0 \times 10^{-1}$	$17.5 \pm 3.5 \times 10^{-1}$	$26.7 \pm 1.9 \times 10^{-1}$	$36.7 \pm 5.2 \times 10^{-1}$	$47.5 \pm 5.5 \times 10^{-1}$
S-BSCF-EC	0	$4.9 \pm 2.9 \times 10^{-2}$	$11.8 \pm 3.0 \times 10^{-1}$	$19.6 \pm 3.1 \times 10^{-1}$	$28.7 \pm 5.8 \times 10^{-1}$	$40.1 \pm 4.5 \times 10^{-1}$	$52.4 \pm 4.5 \times 10^{-1}$

Table C.1 Specific conductivity of $\text{Ba}_{0.5}\text{Sr}_{0.5}\text{Co}_{0.8}\text{Fe}_{0.2}\text{O}_3$ synthesized by sol gel method using various chelating agents

Sample	Specific conductivity, σ (S/cm)						
	550°C	600°C	650°C	700°C	750°C	800°C	σ_{max} (T,°C)
S-BSCF-MC	$53.3 \pm 2.6 \times 10^{-1}$	$44.5 \pm 7.1 \times 10^{-1}$	$39.4 \pm 1.1 \times 10^0$	40.1±0	40.3±0	40.7±0	$53.3 \pm 2.6 \times 10^{-1}$ (550°C)
S-BSCF-G	$46.6 \pm 2.9 \times 10^{-2}$	$53.0 \pm 5.7 \times 10^{-2}$	$45.1 \pm 4.0 \times 10^{-1}$	$43.2 \pm 1.0 \times 10^{-1}$	45.5±0	$45.8 \pm 3.5 \times 10^{-1}$	$53.0 \pm 5.7 \times 10^{-2}$ (600°C)
S-BSCF-H ₅	$47.2 \pm 4.7 \times 10^{-1}$	$42.0 \pm 6.3 \times 10^{-1}$	$39.1 \pm 6.3 \times 10^{-2}$	$38.8 \pm 9.0 \times 10^{-2}$	$38.7 \pm 4.0 \times 10^{-2}$	$39.0 \pm 7.5 \times 10^{-2}$	$47.2 \pm 4.7 \times 10^{-1}$ (550°C)
S-BSCF-GC	$58.6 \pm 2.2 \times 10^{-1}$	$58.7 \pm 5.7 \times 10^0$	$50.1 \pm 6.2 \times 10^{-2}$	49.0±0	$49.0 \pm 1.6 \times 10^{-2}$	$48.0 \pm 3.9 \times 10^{-2}$	$58.7 \pm 5.7 \times 10^{-1}$ (600°C)
S-BSCF-EC	$61.2 \pm 7.2 \times 10^{-1}$	$51.7 \pm 9.5 \times 10^{-1}$	$47.6 \pm 5.5 \times 10^{-2}$	46.9 ± 10^{-2}	$47.0 \pm 4.1 \times 10^{-2}$	$47.5 \pm 2.4 \times 10^{-2}$	$61.2 \pm 7.2 \times 10^{-1}$ (550°C)

Table C.2 Specific conductivity of Ba_{0.5}Sr_{0.5}Co_{0.8}Fe_{0.2}O₃ synthesized by hydrothermal method using various chelating agents

Sample	Specific conductivity, σ (S/cm)						
	27°C	250°C	300°C	350°C	400°C	450°C	500°C
H-BSCF-MC	0	6.7±0	13.4±7.1x10 ⁻²	23.7±2.7x10 ⁻¹	33.1±1.3x10 ⁻¹	44.7±2.9x10 ⁻²	53.4±4.1x10 ⁻¹
H-BSCF-G	0	4.3 ±6.8x10 ⁻²	8.6±2.0x10 ⁻¹	14.8±2.1x10 ⁻¹	22.1±1.1x10 ⁻¹	31.4±5.4x10 ⁻²	40.5±2.0x10 ⁻¹
H-BSCF-H ₅	0	4.0±5.2x10 ⁻²	7.5±4.0x10 ⁻²	12.3±1.2x10 ⁻¹	18.5±9.4x10 ⁻²	25.5±8.2x10 ⁻²	34.6±5.3x10 ⁻²
H-BSCF-GC	0	7.2±1.7x10 ⁻¹	12.4±9.2x10 ⁻²	20.5±1.6x10 ⁻¹	30.8±8.4x10 ⁻¹	41.0±4.5x10 ⁻²	52.9±3.7x10 ⁻²
H-BSCF-EC	0	5.8±8.0x10 ⁻³	10.1±2.1x10 ⁻²	15.8±3.7x10 ⁻²	22.7±2.4x10 ⁻²	30.0±1.4x10 ⁻¹	35.5±5.1x10 ⁻¹

Table C.2 Specific conductivity of Ba_{0.5}Sr_{0.5}Co_{0.8}Fe_{0.2}O₃ synthesized by hydrothermal method using various chelating agents

Sample	Specific conductivity, σ (S/cm)						
	550°C	600°C	650°C	700°C	750°C	800°C	σ_{\max} (T, °C)
H-BSCF-MC	58.0±6.1x10 ⁻¹	44.6±2.4x10 ⁻¹	43.7±2.4x10 ⁻²	45.0±1.9 x10 ⁻³	43.1±1.4x10 ⁻¹	43.0±1.2x10 ⁻¹	58.0±6.1x10 ⁻¹ (550°C)
H-BSCF-G	43.0±6.2x10 ⁻¹	37.0±6.3x10 ⁻¹	34.9±1.3x10 ⁻¹	34.8±9.2x10 ⁻²	35.3±4.3 x10 ⁻³	36.1±2.2x10 ⁻²	43.0±6.2x10 ⁻¹ (550°C)
H-BSCF-H ₅	44.0±1.1x10 ⁻²	45.4±5.3x10 ⁻¹	42.0±1.3x10 ⁻¹	41.6±7.8x10 ⁻²	42.1±2.3x10 ⁻¹	43.1±1.7x10 ⁻¹	45.4±5.3x10 ⁻¹ (600°C)
H-BSCF-GC	55.2±9.7x10 ⁻¹	43.7±7.5x10 ⁻¹	41.2±7.7x10 ⁻²	40.9±1.4x10 ⁻²	41.4±1.5x10 ⁻¹	41.5±1.4x10 ⁻¹	55.2±9.7x10 ⁻¹ (550°C)
H-BSCF-EC	30.2±3.9x10 ⁻¹	29.1±2.2x10 ⁻¹	29.7±1.4x10 ⁻¹	30.3±10 ⁻¹	31.6±2.2x10 ⁻¹	32.4±2.2x10 ⁻¹	35.5±5.1x10 ⁻¹ (500°C)

Table C.3 Specific conductivity of PrSrCoO₄ synthesized by hydrothermal method using various chelating agents

Sample	Specific conductivity, σ (S/cm)						
	27°C	250°C	300°C	350°C	400°C	450°C	500°C
H-PSC-MC	0	$1.5 \pm 4.8 \times 10^{-2}$	$3.1 \pm 8.6 \times 10^{-2}$	$6.3 \pm 1.3 \times 10^{-1}$	$12.4 \pm 1.1 \times 10^{-1}$	$22.5 \pm 1.5 \times 10^{-1}$	$36.9 \pm 4.7 \times 10^{-1}$
H-PSC-G	$0.1 \pm 8.2 \times 10^{-5}$	$2.8 \pm 1.5 \times 10^{-2}$	$6.0 \pm 5.1 \times 10^{-2}$	$10.8 \pm 1.5 \times 10^{-1}$	$19.0 \pm 4.9 \times 10^{-1}$	$31.5 \pm 1.1 \times 10^{-1}$	$50.6 \pm 3.5 \times 10^{-1}$
H-PSC-H ₅	$0.1 \pm 8.5 \times 10^{-5}$	$2.6 \pm 6.1 \times 10^{-2}$	$4.7 \pm 5.5 \times 10^{-2}$	$9.2 \pm 5.5 \times 10^{-2}$	$16.9 \pm 4.5 \times 10^{-1}$	$29.7 \pm 4.3 \times 10^{-1}$	$47.3 \pm 2.9 \times 10^{-1}$
H-PSC-GC	$0.1 \pm 5.1 \times 10^{-4}$	$1.5 \pm 8.3 \times 10^{-2}$	$3.3 \pm 9.9 \times 10^{-2}$	$6.7 \pm 7.6 \times 10^{-2}$	$13.0 \pm 1.0 \times 10^{-1}$	$23.5 \pm 3.4 \times 10^{-2}$	$39.2 \pm 1.4 \times 10^{-1}$
H-PSC-EC	0	$2.2 \pm 5.3 \times 10^{-2}$	$4.1 \pm 3.9 \times 10^{-2}$	$7.3 \pm 3.9 \times 10^{-2}$	$13.6 \pm 7.7 \times 10^{-3}$	$25.2 \pm 1.9 \times 10^{-1}$	$41.9 \pm 6.3 \times 10^{-2}$

Table C.3 Specific conductivity of PrSrCoO₄ synthesized by hydrothermal method using various chelating agents

Sample	Specific conductivity, σ (S/cm)						
	550°C	600°C	650°C	700°C	750°C	800°C	σ_{\max} (T,°C)
H-PSC-MC	$54.4 \pm 2.9 \times 10^{-2}$	$74.3 \pm 4.9 \times 10^{-2}$	$97.0 \pm 2.5 \times 10^{-1}$	$123.9 \pm 5.5 \times 10^{-1}$	150.3 ± 1.2	$172.7 \pm 5.9 \times 10^{-1}$	$172.7 \pm 5.9 \times 10^{-1}$ (800°C)
H-PSC-G	$72.6 \pm 1.4 \times 10^{-1}$	95.1 ± 3.1	$127.9 \pm 1.7 \times 10^{-1}$	$159.3 \pm 4.4 \times 10^{-1}$	$183.8 \pm 5.3 \times 10^{-1}$	$202.6 \pm 4.2 \times 10^{-1}$	$202.6 \pm 4.2 \times 10^{-1}$ (800°C)
H-PSC-H ₅	$70.5 \pm 7.8 \times 10^{-2}$	$96.6 \pm 3.4 \times 10^{-1}$	$125.0 \pm 3.2 \times 10^{-1}$	$151.8 \pm 5.2 \times 10^{-1}$	$174.6 \pm 3.6 \times 10^{-1}$	$192.8 \pm 2.2 \times 10^{-1}$	$192.8 \pm 2.2 \times 10^{-1}$ (800°C)
H-PSC-GC	$60.5 \pm 3.3 \times 10^{-1}$	$86.5 \pm 1.7 \times 10^{-1}$	$115.3 \pm 5.1 \times 10^{-1}$	$141.0 \pm 3.8 \times 10^{-2}$	163.8 ± 0	$181.5 \pm 5.4 \times 10^{-2}$	$181.5 \pm 5.4 \times 10^{-2}$ (800°C) ¹
H-PSC-EC	$63.5 \pm 3.5 \times 10^{-2}$	$89.1 \pm 1.5 \times 10^{-1}$	$118.5 \pm 4.3 \times 10^{-1}$	$146.3 \pm 4.4 \times 10^{-2}$	$168.6 \pm 6.4 \times 10^{-2}$	$186.5 \pm 2.1 \times 10^{-1}$	$186.5 \pm 2.1 \times 10^{-1}$ (800°C)

Table C.4 Specific conductivity of PrSrNiO₄ synthesized by hydrothermal method using various chelating agents

Sample	Specific conductivity, σ (S/cm)						
	27°C	250°C	300°C	350°C	400°C	450°C	500°C
H-PSN-MC	$319.7 \pm 1.2 \times 10^{-1}$	$193.1 \pm 6.6 \times 10^{-1}$	$221.3 \pm 7.6 \times 10^{-1}$	236.5 ± 1.0	238.3 ± 6.7	229.3 ± 0	$228.7 \pm 2.9 \times 10^{-1}$
H-PSN-G	278.2 ± 1.4	$205.6 \pm 2.2 \times 10^{-1}$	$206.5 \pm 7.3 \times 10^{-1}$	$205.9 \pm 1.9 \times 10^{-1}$	200.6 ± 0	$187.5 \pm 3.8 \times 10^{-1}$	191.7 ± 2.1
H-PSN-H ₅	$593.5 \pm 1.4 \times 10^{-1}$	$431.2 \pm 3.6 \times 10^{-1}$	$420.1 \pm 3.0 \times 10^{-1}$	$400.4 \pm 1.1 \times 10^{-1}$	395.1 ± 4.2	$380.6 \pm 5.9 \times 10^{-1}$	359.6 ± 1.7
H-PSN-GC	$358.0 \pm 1.3 \times 10^{-1}$	$108.8 \pm 4.5 \times 10^{-1}$	125.0 ± 1.2	$135.9 \pm 8.2 \times 10^{-1}$	133.2 ± 0	$119.8 \pm 6.3 \times 10^{-1}$	120.4 ± 2.5
H-PSN-EC	856.0 ± 6.7	$624.8 \pm 1.6 \times 10^{-13}$	604.6 ± 0	595.3 ± 0	573.1 ± 0	551.6 ± 6.1	$528.2 \pm 1.1 \times 10^{-1}$

Table C.4 Specific conductivity of PrSrNiO₄ synthesized by hydrothermal method using various chelating agents

Sample	Specific conductivity, σ (S/cm)						
	550°C	600°C	650°C	700°C	750°C	800°C	σ_{\max} (T, °C)
H-PSN-MC	$228.7 \pm 2.9 \times 10^{-1}$	$232.3 \pm 9.9 \times 10^{-1}$	$237.0 \pm 4.2 \times 10^{-1}$	$238.2 \pm 7.6 \times 10^{-1}$	239.9 ± 1.4	215.8 ± 1.1	$319.7 \pm 1.2 \times 10^{-1}$ (27°C)
H-PSN-G	188.3 ± 0	197.2 ± 0	$200.9 \pm 7.6 \times 10^{-1}$	203.2 ± 1.6	$202.4 \pm 8.2 \times 10^{-1}$	$204.7 \pm 6.7 \times 10^{-1}$	278.2 ± 1.4 (27°C)
H-PSN-H ₅	346.4 ± 3.8	332.4 ± 0	324.2 ± 0	311.8 ± 1.5	310.6 ± 3.2	304.4 ± 0	$593.5 \pm 1.4 \times 10^{-1}$ (27°C)
H-PSN-GC	119.3 ± 1.4	$114.4 \pm 6.6 \times 10^{-1}$	$125.2 \pm 3.7 \times 10^{-1}$	$137.5 \pm 5.5 \times 10^{-1}$	$149.7 \pm 8.7 \times 10^{-1}$	161.7 ± 1.0	$358.0 \pm 1.3 \times 10^{-1}$ (27°C)
H-PSN-EC	$504.9 \pm 8.3 \times 10^{-1}$	486.4 ± 1.3	$464.2 \pm 2.6 \times 10^{-1}$	$448.0 \pm 8.2 \times 10^{-1}$	442.3 ± 2.4	436.6 ± 0	856.0 ± 6.7 (27°C)

Table C.5 Specific conductivity of $\text{La}_{0.7}\text{Sr}_{0.3}\text{Ga}_{0.7}\text{Fe}_{0.2}\text{Mg}_{0.1}\text{O}_3$ synthesized by hydrothermal method using various chelating agents

Sample	Specific conductivity, σ (S/cm)						
	27°C	250°C	300°C	350°C	400°C	450°C	500°C
H-LSGFM-MC	0	0	$0.01 \pm 6.7 \times 10^{-5}$	$0.02 \pm 5.2 \times 10^{-5}$	$0.03 \pm 3.3 \times 10^{-5}$	$0.05 \pm 4.3 \times 10^{-4}$	$0.07 \pm 1.5 \times 10^{-4}$
H-LSGFM-GC	0	0	$0.01 \pm 2.6 \times 10^{-4}$	$0.02 \pm 2.6 \times 10^{-4}$	$0.03 \pm 1.6 \times 10^{-4}$	$0.05 \pm 4.2 \times 10^{-4}$	$0.07 \pm 9.1 \times 10^{-4}$

Sample	Specific conductivity, σ (S/cm)						
	550°C	600°C	650°C	700°C	750°C	800°C	σ_{\max} (T, °C)
H-LSGFM-MC	$0.09 \pm 2.2 \times 10^{-4}$	$0.13 \pm 9.2 \times 10^{-5}$	$0.17 \pm 2.8 \times 10^{-4}$	$0.22 \pm 7.0 \times 10^{-4}$	$0.26 \pm 9.3 \times 10^{-4}$	$0.26 \pm 3.0 \times 10^{-3}$	$58.0 \pm 6.1 \times 10^{-1}$ (550°C)
H-LSGFM-GC	$0.11 \pm 1.5 \times 10^{-3}$	$0.14 \pm 2.4 \times 10^{-4}$	$0.18 \pm 4.7 \times 10^{-4}$	$0.23 \pm 6.1 \times 10^{-4}$	$0.39 \pm 7.9 \times 10^{-4}$	$0.32 \pm 7.4 \times 10^{-3}$	$43.0 \pm 6.2 \times 10^{-1}$ (550°C)

Table C.6 Specific conductivity of $\text{La}_{0.8}\text{Sr}_{0.2}\text{Ga}_{0.8}\text{Mg}_{0.15}\text{Co}_{0.05}\text{O}_{3-\delta}$ synthesized by hydrothermal method using various chelating agents

Sample	Specific conductivity, σ (S/cm)						
	27°C	250°C	300°C	350°C	400°C	450°C	500°C
H-LSGCM-MC	0	0	0	0	0	0	0

Sample	Specific conductivity, σ (S/cm)						
	550°C	600°C	650°C	700°C	750°C	800°C	σ_{max} (T, °C)
H-LSGCM-MC	0	0	$0.01 \pm 3.6 \times 10^{-5}$	$0.01 \pm 1.4 \times 10^{-8}$	$0.02 \pm 6.8 \times 10^{-4}$	$0.02 \pm 9.1 \times 10^{-5}$	$58.0 \pm 6.1 \times 10^{-1}$ (550°C)

VITAE

Miss Ratchanit Hiri-o-tuppa was born on February 28, 1984 in Chonburi, Thailand. She graduated with Bachelor's Degree in Petrochemicals and Polymeric Materials from Faculty of Engineering and Industrials Technology, Silpakorn University in 2006. She continued her study in Petrochemistry and Polymer Science Program, Faculty of Science, Chulalongkorn University in 2006 and completed in 2009.